Radiation-induced cancer risk and decision-making in a simulated Cs-137 urban event

Edson R. Andrade ,
Renato G. Gomes,
Ricardo Stenders,
Tercio Brum,
Sergio X. Lima,
Mariana S. C. Castro,
Ademir X. Silva

Abstract. The triggering of a "dirty bomb" generates a complex scenario, with enormous challenges for the responders due to initial misinformation and the urgency to act quickly yet effectively. Normally, the first 100 h are decisive for perceiving the risk in a more realistic dimension, but the support of methodologies that rely on computational simulations can be valuable when making key decisions. This work seeks to provide support for the early decision-making process by using a Gaussian model for the distribution of a quantity of Cs-137 spread by a radiological dispersive device (RDD). By sequentially joining two independent programs, HotSpot Health Physics codes and RESidual RADiation (RESRAD)-RDD family of codes, we came up with results that suggest a segmented approach to the potentially affected population. These results advocate that (a) the atmospheric stability conditions represented by the Pasquill–Gifford classes and (b) the population subgroups defined by radiation exposure conditions strongly influence the postdetonation radiological effects. These variables should be taken into account in the elaboration of flexible strategies that include many climatic conditions and to prioritize attention to different groups of public at risk. During the initial phases of such an event, it is believed that simulations using Gaussian models may be of value in anticipating the possible changes in key variables during the decision-making process. These variables may severely affect the effectiveness of the actions of responders and the general public's safety.

Keywords: Environmental contamination • Dispersive device • Decision-making

E. R. Andrade
IBMEC, Faculty of Engineering, Graduate Program
Rio de Janeiro, Brazil
and Nuclear Engineering Graduate Program
Federal University of Rio de Janeiro (COPPE/UFRJ)
Rio de Janeiro, Brazil
and Defense Engineering Graduate Program
Military Institute of Engineering
Praça General Tibúrcio 80, Rio de Janeiro, Brazil
E-mail: fisica.dna@gmail.com

R. G. Gomes, A. X. Silva
Nuclear Engineering Graduate Program
Federal University of Rio de Janeiro (COPPE/UFRJ)
Rio de Janeiro, Brazil

R. Stenders
IBMEC, Faculty of Engineering, Graduate Program
Rio de Janeiro, Brazil

T. Brum, S. X. Lima, M. S. C. Castro
Defense Engineering Graduate Program
Military Institute of Engineering
Rio de Janeiro, Brazil

Introduction

Recent scientific efforts have shown that simulations of events that may be hazardous to the population are a useful and effective tool to estimate exposure to radiation [1–5]. Nevertheless, limited access to the needed information about an event may negatively affect the effectiveness of this methodology.

This work aims to assess the radiological risk caused by activation of a radiological dispersive device (RDD), colloquially referred to as a "dirty bomb" [5–7]. The RDD is a hypothetical weapon that combines radioactive material with conventional explosives [1]. The main goal of this device is to spread radiation across an inhabited area, thus creating social and public health risks [3, 4, 8, 9]. Two independent computer programs were used in tandem; by applying the HotSpot Health Physics software [10], the event scenario was assembled. Then, the ground surface data were used as the input for the RESidual RADiation (RESRAD)-RDD software [11], which translated it into radiation dose. This information is essential when evaluating the extension of radiological risk over a target population or area.

The main idea of this work is to explore the influence of the Pasquill–Gifford atmospheric stability

classes (PG stability classes) [12] on radiological risks and decision-making. The changes in the PG stability classes may affect the radiation dose from activation of an RDD and, ultimately, increase the risk of developing illnesses such as radiation-induced cancer. For this work, leukemia was chosen as the representative illness due to its latency period. The risk of developing leukemia is used in this study as the target consequence. The correlation between leukemia risk and changes in PG stability classes was evaluated based on the fact that radioactive contamination is displayed at the ground level, which is addressed as ground shine exposure.

Generally, a risk evaluation involves a number of uncertainties, which should be taken into account when estimating the results, usually as confidence intervals. This study considers that the main uncertainties related to the radiological risk represented by development of radiation-induced leukemia are taken into account by the incidence model [13, 14]. Therefore, a discussion about the sources of uncertainty for evaluating the risk of development of leukemia falls beyond the scope of this work.

The major expected contribution from this work is to provide fast and essential information about future developments of an event. This information may help decision-makers to improve their response strategy. The contamination plumes were designed considering some selected reference levels, namely, those for acute radiation syndrome (ARS), evacuation, and sheltering [15]. An urban environment was considered for the event scenario. The main goal then is to show that changes in the PG stability classes should be considered a factor that is able to change the risk levels. Such changes may urge new prioritization criteria based on the radiological risk posed by the total effective dose equivalent (TEDE) of radiation on a potentially affected population.

From a particular perspective, changes in the local environmental conditions may represent an important source of variability for assessing the TEDE and the consequent radiological risk. By comparing the findings, an assessment including the differences in the PG stability classes may aid decision-makers in producing pertinent solutions. Overall, the results suggest that all groups are under a specific risk and should be treated in a different manner. Such a complex scenario that demands fast assessment of the information available may be facilitated by such a methodology.

Materials and methods

The radiological event was simulated by activating a hypothetical RDD, which in turn was expected to produce an off-site radiological contamination. The release may produce radiation-based ground surface contamination, thus generating an environmental radiation dose. This work considers this radiation dose as the key factor for evaluating the radiological risk. Ground contamination was simulated using HotSpot Health Physics codes 3.1.1 [10], and the results were measured (simulated) in picocurie per square meter (pCi/m²). Then, the ground contamina-

tion was used as the input for RESRAD-RDD, which converts all values in radiation doses (measured in rem [Roentgen equivalent men]) into sieverts. The RESRAD-RDD model assumes that an RDD event occurs outdoors and contaminates the streets, the soil, exterior walls, roofs of buildings, interior walls, and floors of buildings with radioactive material.

The ground contamination simulated by HotSpot is a Gaussian plume model (refer to Eq. (1)). This model is convenient since it runs fast, allowing the estimation of the concentrations at any point in a 3D space [10].

$$(1) \quad C(x,y,z,H) = \frac{Q}{2\pi\sigma_y\sigma_z u}\exp\left[-\frac{1}{2}\left(\frac{y}{\sigma_y}\right)^2\right]$$

$$\cdot\left\{\exp\left[-\frac{1}{2}\left(\frac{z-H}{\sigma_z}\right)^2\right]\right\}$$

$$+\exp\left[-\frac{1}{2}\left(\frac{z+H}{\sigma_z}\right)^2\right]\exp\left[-\frac{\lambda x}{u}\right]\cdot DF(x)$$

where C is the time-integrated atmospheric concentration (in curie-seconds per cubic meter [Ci-s/m³]); Q is the source term (in curies); H is the effective release height (in meters); λ is the radioactive decay constant (per second [s⁻¹]); x, y, and z are the downwind, crosswind, and vertical distances (in meters), respectively; σ_y and σ_z are the standard deviations (SD) of the integrated concentration distributions in the cross-wind and vertical directions (in meters), respectively; u is the average wind velocity at the effective release height (in meters per second [m/s]), and $DF(x)$ is the plume depletion factor.

HotSpot takes into account the wind velocity and the local atmospheric stability class. The local environmental stability conditions were considered as follows: (A) extremely unstable; and (F) moderately stable [10].

The atmospheric stability can be defined as the tendency of an amount of air to move downward and upward after a vertical displacement. Essentially, the unstable class (PG stability Class A) tends to develop vertical updrafts, which increase the turbulence intensity of the boundary layers. On the other hand, the stable class (PG stability Class F) tends to suppress vertical updrafts, reducing turbulence intensity [12]. Table 1 summarizes the earliest stability classification scheme, known as Pasquill–Gifford stability classes, which requires solely an estimate of the wind velocity and the local insulation [12].

The following major results from the simulations were evaluated: (a) the arrival time; (b) the con-

Table 1. Meteorological conditions for determination of atmospheric stability classes [10]

Wind velocity [m/s]	High insulation	Low insulation	Night time
<2	A	B	F
2–3	A	C	E
3–4	B	C	D
4–6	C	D	D
>6	C	D	D

tamination plume area and the potentially affected population; (c) the ground shine and TEDE; and (d) the subgroup radiological risk.

Normally, in an event potentially involving an RDD, any of the 11 most likely radionuclides expected to be used can be considered. The main list of potential radionuclides includes Am-241, Cf-252, Cm-244, Co-60, Cs-137, Ir-192, Po-210, Pu-238, Pu-239, Ra-226, and Sr-90 [11]. For this study, the source term Cs-137 was chosen due to its solubility and the highly dispersible emission of penetrating radiation [11]. Cs-137 is produced by fission in a nuclear reactor and has a half-life of about 30 years.

The main HotSpot input data for the calculations were as follows: (a) source material: Cs-137; (b) material at risk: 3.7×10^{15} Bq; (c) wind speed: 2 m/s; (d) high explosive: 10 pounds of TNT; (e) stability class: A and F, considering Class A as extremely unstable and Class F as moderately stable; (f) receptor height from the ground: 10 m; (g) distance coordinates: all distances are measured along the centerline of the plume for 0.5, 1, 2, 4, 6, 8, and 10 km. There are no special reasons for the distances along the plume centerline, except for 10 km. The HotSpot model is recommended by the developers for those simulations that consider distances up to a maximum of 10 km from the release point due to the uncertainties raised. This work does not account for blast damage and mechanical risk from the RDD explosion.

The plume boundaries were defined by considering the reference levels, which are limited to the contamination plume boundaries. The reference levels are as follows: 700 mSv, for acute radiation syndrome (ARS) [16], limited to the inner boundary; 50 mSv, for evacuation [15], limited to the middle boundary; and 10 mSv for sheltering [15], limited to the outer boundary of plume contamination. The TEDE is defined as the radioactive material producing the dose equivalent by external and/or internal exposure. The TEDE is the most comprehensive expression of the combined dose from all delivery pathways [10].

The RESRAD-RDD code is designed to attempt operational guidelines, which are organized into seven groups [11]. Furthermore, these groups are divided into subgroups, generally categorized by the phase of emergency response. The main groups A–G are as follows: (a) Group A – access control during emergency response operations; (b) Group B – early-phase protective action; (c) Group C – relocation from different areas and critical infrastructure utilization in relocation areas; (d) Group D – temporary access to relocation areas for essential activities; (e) Group E – transportation and access routes; (f) Group F – release of property from radiologically controlled areas; and (g) Group G – food consumption.

The results from HotSpot are entered into RESRAD-RDD, which in turn calculates the radiation doses (TEDE) for the B subgroups. It is assumed that only the outdoor ground surface, which has an infinitely large area, is contaminated. The study is focused on the early-phase protective action (evacuation or sheltering) within 4 d (96 h) after the event. Therefore, the operational guidelines may help decision-makers perform time-sensitive decisions. Table 2 shows the definitions of each B subgroup [11]. The radiation doses received by the subgroups B1-1, B1-2, and B1-3 are considered by RESRAD-RDD, as described in Table 2 [11].

The next step is inserting these radiation doses in the equations of the Biological Effects of Ionizing Radiation V (BEIR V) method [17] in order to evaluate the risks. An estimate of the risk of fatal cancer development for a given population was performed according to Eq. (2) [13, 14, 17].

$$(2) \qquad \gamma(d) = \gamma_0 + f(d)\,g(\beta)\,\gamma_0$$

where γ_0 is the age- and sex-specific mortality rate in the absence of radiation exposure more than the natural background [18]; $g(\beta)$ is the excess risk function for a specific cancer (this function depends upon sex, age, age at the time of exposure, and time since exposure); and $\gamma(d)$ represents the total fatal risk. The second term in Eq. (2), the term "$f(d)g(\beta)\gamma_0$", where the variable "d" is the TEDE from the RESRAD-RDD software calculations for each B subgroup, represents the radiation-induced risk of fatal cancer. In this study, the values for γ_0 were taken

Table 2. Definitions for each B subgroup [11]

Subgroup	Description
B1-1 (resident spending time indoors)	Assumes that the outside ground surface is contaminated and that the resident spends 100% of the time indoors. Radiation doses are from (a) exposure to external radiation from contaminated surfaces, (b) inhalation of contaminated air, and (c) exposure to external radiation from submersion in contaminated air.
B1-2 (resident spending time both indoors and outdoors)	Assumes that the resident spends 16.4 h/d indoors and 7.6 h/d outdoors. Radiation doses are from (a) exposure to external radiation from contaminated surfaces, (b) exposure to external radiation from the contaminated ground surface, (c) inhalation of internal contaminated air, (d) inhalation of external contaminated air, (e) exposure to external radiation from submersion in indoor contaminated air, (f) exposure to external radiation from submersion in outdoor contaminated air, and (g) ingestion of contamination deposited on the ground surface.
B1-3 (worker spending time outdoors)	Assumes that the worker spends 100% of the time outdoors. Radiation doses are from (a) exposure to external radiation from the contaminated ground surface, (b) inhalation of contaminated air, (c) exposure to external radiation from submersion in contaminated air, and (d) ingestion of contamination deposited on the ground surface.

Table 3. Equations for estimating leukemia (male and female) [14]

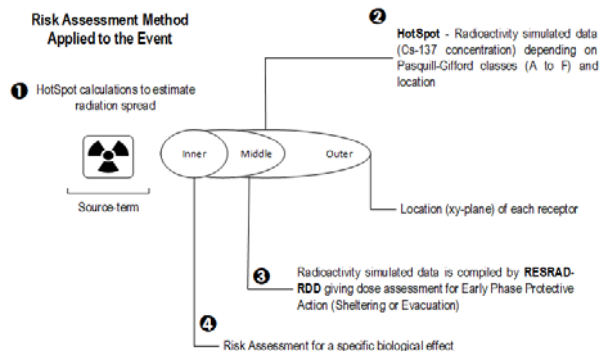| Range of T	Equation	
$E \leq 20$; $T \leq 15$	$g(\beta) = \exp(4.885) = 132.3$	(4a)
$E \leq 20$; $15 < T \leq 25$	$g(\beta) = \exp(2.38) = 10.8$	(4b)
$E > 20$; $T \leq 25$	$g(\beta) = \exp(2.37) = 10.7$	(4c)
$E \leq 20$; $25 < T \leq 30$	$g(\beta) = \exp(1.638) = 5.14$	(4d)

Fig. 1. Simplified scheme of the work methodology.
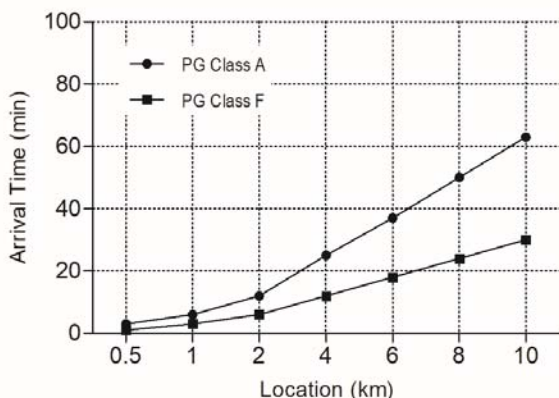
Fig. 2. Contamination plume arrival time at each location and PG stability classes A and F.

as $5.75/10^5$ individuals and $4.56/10^5$ individuals for males and females, respectively. This information is based on the Brazilian population being used only for exemplification purposes [18].

The functions $g(\beta)$ are studied by groups for leukemia and have mathematical formulations shown by Eqs. (4a)–(4d) in Table 3. In $g(\beta)$ equations, the variable E represents the age at exposure, and T is

the time in years following exposure. The latency for leukemia was considered as 2 years [14].

The potentially affected population was estimated by multiplying the contamination plume area and the local population density, resulting in a provisional quantity named population-area. Figure 1 summarizes the main ideas and methodology steps.

Results

Figure 2 shows the difference in arrival time of the contamination plume when PG classes A and F are compared to each other. The arrival time is the time expected for the radioactive plume to arrive at a specific location after the detonation of the RDD.

Figure 3 (A and B) shows the calculations for ground shine and TEDE, respectively, for each location within the contamination plume, with panels A and B showing the results for PG classes A and F.

Figure 4 shows the estimation for area and the population-area for all contamination plume boundaries (inner, middle, and outer) and PG classes A and F.

Figure 5 shows the TEDE calculations for each location within the contamination plume. Part figure 5A and 5B show the results for all RESRAD-RDD subgroups B1-1, B1-2, and B1-3 considering PG classes A and F, respectively.

Figure 6 shows the fatal radiation-induced risks for leukemia considering all RESRAD-RDD B subgroups (B1-1, B1-2, and B1-3) as a function of the receptor location, sex, age group, and PG classes (A and F). The risks for the subgroups developing leukemia within 2 years are presented. The information contained in Fig. 6 is related to the BEIR V equations, and the values are functions of the receiver location, sex, age group, and PG classes (A and F). For its evaluation, it should be considered that each subgroup is subject to a risk assessment that includes the functions $g(\beta)$, which are divided into four groups (T1, T2, T3, and T4) according to the time since the exposure.

Discussion

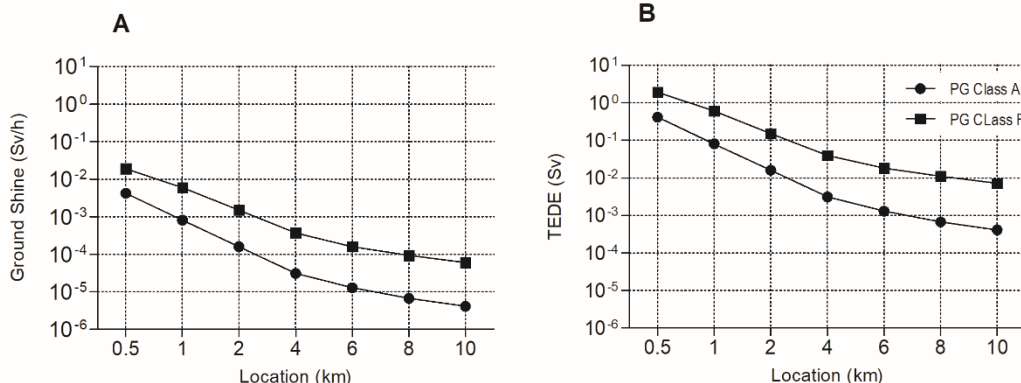Figure 2 shows the comparison between the times of arrival of the plumes at each location for both

Fig. 3. Ground shine dose rate and TEDE for each location. Panels A and B show results for PG stability classes A and F.
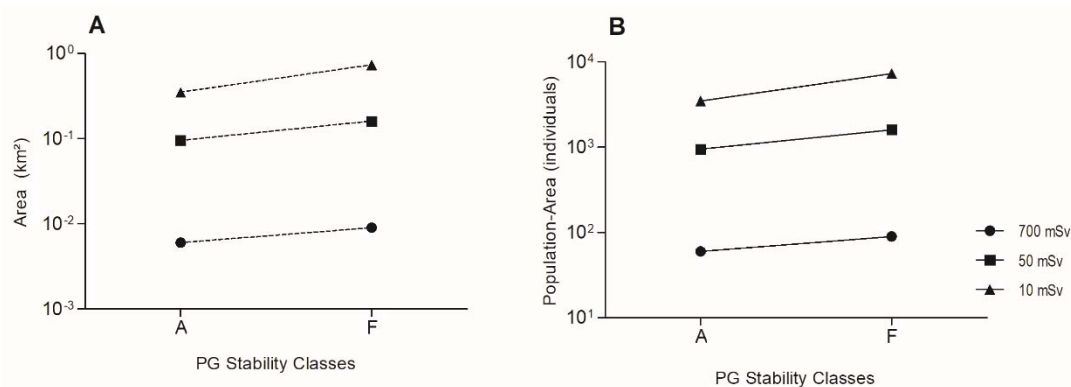
Fig. 4. Estimations of the area and the population-area. Panels A and B show results for the PG stability classes A and F.
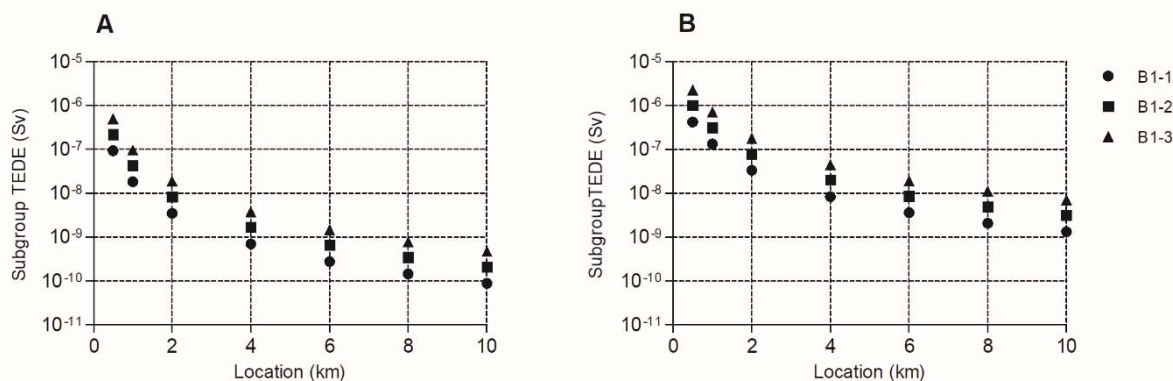

Fig. 5. TEDE calculations for the three subgroups. Part figures 5A and 5B show the results for all subgroups B1-1, B1-2, and B1-3 considering PG classes A and F, respectively.

PG classes A and F. This result allows inferring that changes from Class A to Class F may raise the radiological risk levels. This is due to the anticipation of the exposure, which affects the timing of the response and the sheltering procedures. This new subevent implies the need for improvements in the risk communication process.

The ground shine dose rate and TEDE are results that are complementary; hence, exposure to ground shine is one of the components of the total TEDE calculation. Figure 3 suggests that both results (TEDE and ground shine) are influenced by changes in the PG classes. This fact can generate an impact on the logistics of the response because the results can change how long one must stay at a contaminated location in order to reach a certain limit of the reference dose of radiation. Therefore, changes in dose rates should be considered as resulting from both a change in the receptor position and the possible changes in PG classes. This condition ends up having an impact on the overall radiological risk.

Figure 4 presents an important finding that suggests that there are variations in the areas of the plumes and, consequently, in the sizes of the potentially affected population. These variations are perceived in the slopes of the curves in the graphs, with more emphasis on the individuals under shelter conditions (10 mSv). As can be seen, a variation from Class A to Class F can cause a significant change in the number of individuals passing from the evacuation group to the sheltering group. In this specific case, regarding the logistics of the

evacuation operation, the impact may be positive. The expected result is a reduction in the number of individuals involved. Nevertheless, this process of changing PG stability classes is slow. Updating the conditions and implications must be done in real time in order to update the procedures. This might allow decision-makers some time to be able to change or update their plan of action.

Figure 5 illustrates a simulation of the behaviour of TEDE by subgroup. Figure parts 5A and 5B refer, respectively, to PG stability classes A and F for subgroups B1-1, B1-2, and B1-3. From the results, it can be inferred that the subgroup B1-3 is more affected and faces a worsened condition when it experiences a change of PG class (from A to F). This behaviour is present, in a similar form, for all the subgroups, although, in subgroup B1-3, it is present in a "heightened" manner. It may be suggested that the subgroup B1-3 be monitored and its constitution established based on the risk predicted by the simulations, taking into consideration the time (in years) following exposure for the responders. In the case of leukemia, the equations do not show significant differences for the values of the $g(\beta)$ functions when the variable sex is changed [13, 14]. This behaviour can be verified by comparing the results presented in the panels 6A (females), 6B (males), 6C (females), and 6D (males).

More comprehensive evaluations may be made from the results shown in Fig. 6. This analysis might be interesting for decision-making considering all the factors in the scenario. The data presented suggest
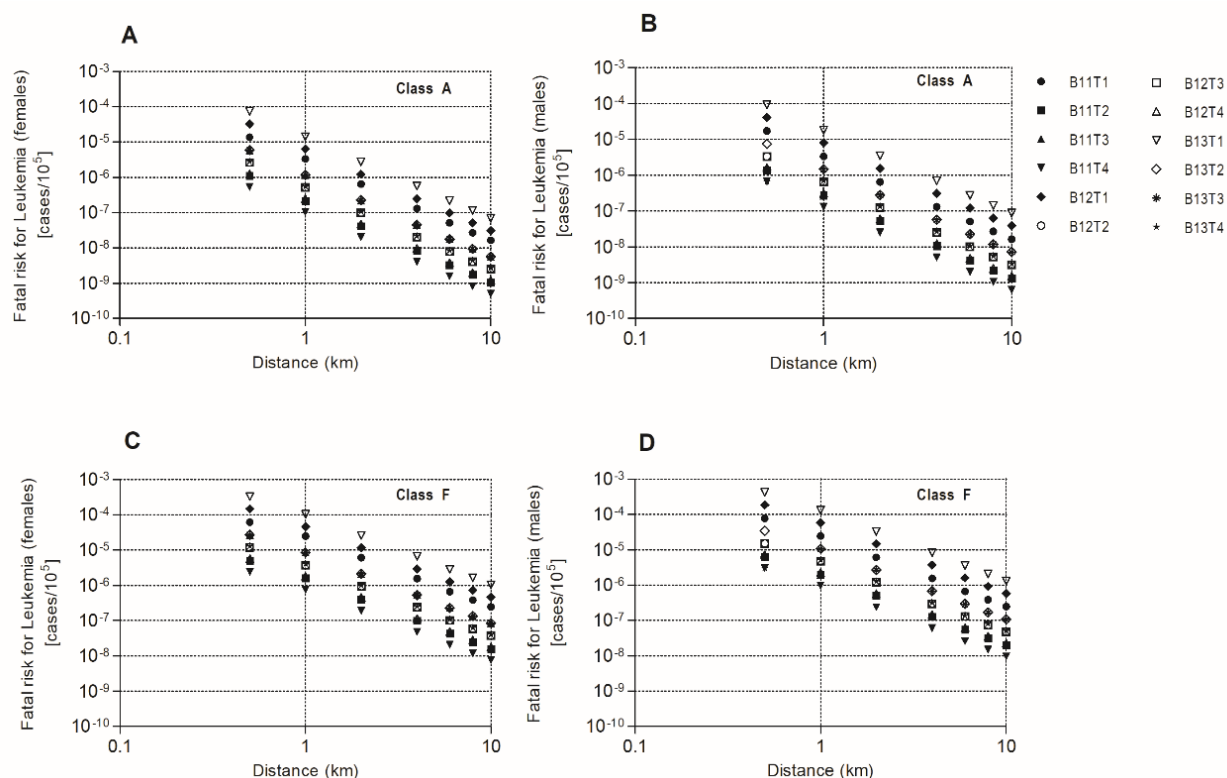
Fig. 6. Fatal radiation-induced risks for leukemia.

an increase in the risk of developing leukemia in the case of variation from PG Class A to Class F. Within each PG class's subgroup, there seems to be a strong risk interaction with the time group, as expected; the distance factor attenuates all risks regardless of PG stability class and subgroup.

The interaction between age and risk of developing leukemia may be a positive impact factor in the constitution of teams for the B1-3 subgroup. In all cases, the level of risk increases approximately by an order of magnitude on varying the PG stability class from A to F, regardless of the sex.

Conclusion

This study aimed to show how computational simulation of radiological events in urban environments assists the authorities. The simulation was successful in performing the evaluation in two independent stages using two different computational programs. The HotSpot code was used to create an event that generated the data of interest. Second, the results were inserted into the RESRAD-RDD software, and the generated data allowed the successful evaluation of the risk of developing fatal leukemia for each subgroup B1-1, B1-2, and B1-3. Variables such as sex, age, location, and PG class were included in this evaluation.

From the results, it can be inferred that there are differences in the risks between the considered subgroups. The simulation is of importance for both assessing risk and defining logistic aspects. Moreover, the establishment of response actions that take into account possible climate changes may be suggested. In

this perspective, it is expected that this work can support decision-making in a critical environment, hence generating positive effects in logistics and ensuring the protection of response teams and the public.

ORCID

Edson R. Andrade http://orcid.org/0000-0001-8800-6105

References

1. Rother, F. C., Rebello, W. F., Healy, M. J. F., Silva, M. M., Cabral, P. A. M., Vital, H. C., & Andrade, E. R. (2016). Radiological risk assessment by convergence methodology model in RDD scenarios. *Risk Anal.*, *36*(11), 2039–2046.
2. Andrade, C. P., Souza, C. J., Camerini, E. S. N., Alves, I. S., Vital, H. C., Healy, M. J. F., & De Andrade, E. R. (2018). Support to triage and public risk perception considering long-term response to a Cs-137 radiological dispersive device scenario. *Toxicol. Ind. Health*, *34*(6), 433–438.
3. Jeong, H., Park, M., Jeong, H., Hwang, W., Kim, E., & Han, M. (2013). Radiological risk assessment caused by RDD terrorism in an urban area. *Appl. Radiat. Isot.*, *79*, 1–4.

4. Porter, K., & Lee, L. (2007). Radiological terrorism scenarios. *Prehosp. Disaster Med.*, *22*(6), 547.

5. Harper, F. T., Musolino, S. V., & Wente, W. B. (2007). Realistic radiological dispersal device hazard boundaries and ramifications for early consequence management decisions. *Health Phys.*, *93*(1), 1–16.

6. Mettler, F. A. Jr. (2005). Medical resources and requirements for responding to radiological terrorism. *Health Phys.*, *89*(5), 488–493.

7. Conklin, C., & Edwards, J. (2000). Selection of protective action guides for nuclear incidents. EPA. *J. Hazard. Mater.*, *75*(2/3), 131–144.

8. Timins, J. K., & Lipoti, J. A. (2004). Radiological terrorism. *N. J. Med.*, *101*(Suppl. 9), 66–75; quiz 75–76.

9. Stone, R. (2002). Radiological terrorism. New effort aims to thwart dirty bombers. *Science*, *296*(5576), 2117–2119.

10. Homann, S. G., & Aluzzi, F. (2019). *HotSpot Health Physics Codes Version 3.0 User's Guide*. Lawrence, CA, USA: Livermore National Laboratory.

11. Yu, C. (2009). *Preliminary report on operational guidelines developed for use in emergency preparedness and response to a radiological dispersal device incident*. Chicago: Argonne National Laboratory.

12. Pasquill, F. (1961). The estimation of the dispersion of windborne material. *Meteorol. Mag.*, *90*(1063), 33–41.

13. Maillie, H. D., Simon, W., Watts, R. J., & Quinn, B. R. (1993). Determining person-years of life lost using the BEIR V method. *Health Phys.*, *64*(5), 461–466.

14. Maillie, H. D., & Jacobson, A. P. (1992). A graphical method of estimating fatal radiation-induced cancers using the BEIR V method. *Health Phys.*, *63*(3), 273–280.

15. ICRP. (1977). Implications of Commission recommendations that doses be kept as low as readily achievable. In *A report of ICRP Committee 4* (pp. 2–3). Oxford. (ICRP Publication 22).

16. Institute of Medicine. (1999). Follow-up of persons with known or suspected exposure to ionizing radiation. In *Potential radiation exposure in military operations: Protecting the soldier before, during, and after* (pp. 88–107). Washington, DC: The National Academies Press. Available from https://doi.org/10.17226/9454.

17. IAEA. (1996). *Methods for estimating the probability of cancer from occupational radiation exposure*. Vienna: International Atomic Energy Agency. (IAEA-TECDOC-870).

18. INCa. (2018). *Estimate/2018 – Cancer incidence in Brazil*. Rio de Janeiro: Instituto Nacional de Câncer José Alencar Gomes da Silva.